JCTC Journal of Chemical Theory and Computation

Article

pubs.acs.org/JCTC

Mechanisms for Solvatochromic Shifts of Free-Base Porphine Studied with Polarizable Continuum Models and Explicit Solute−Solvent Interactions

Ryoichi Fukuda*,†,‡ and Masahiro Ehara†,‡

†Department of Theoretical and Computational Molecular Science, Institute for Molecular Science and Research Center for Computational Science, 38 Nishigo-Naka, Myodaiji, Okazaki 444-8585, Japan

‡Japan Science and Technology Agency CREST, Sanboncho-5, Chiyoda-ku, Tokyo 102-0075, Japan

Supporting Information

ABSTRACT: Solvatochromic shifts of free-base porphine in the Q-band and B-band were studied using the polarizable continuum model (PCM) and explicit solvent molecules employing time-dependent density functional theory (TDDFT) and the symmetry-adapted cluster-configuration interaction (SAC-CI) method. The state-specific (SS) and linear-response (LR) methods were examined in the PCM calculations. These models involve different types of solute−solvent interactions. The LR PCM and explicit solvation models reproduced the experimentally observed trends of the solvatochromic shifts, while the SS PCM failed to reproduce the experimental findings. The origin of the solvatochromic shifts of free-base porphine was dispersive interactions between the solute and solvent. Specific solute−solvent interactions would be important for a decrease of the splitting width between Q-bands. Based on the Casimir−Polder formula and a decomposition analysis, it was found that the dominant part of the solute−solvent interactions can be considered using independent particle approximations.

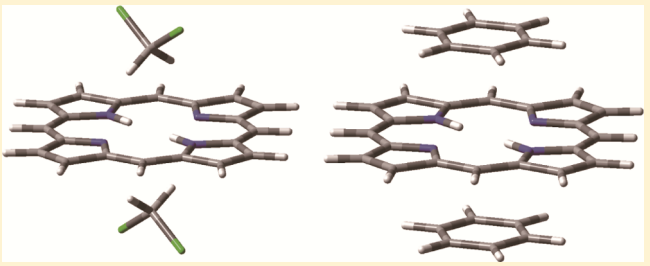

1. INTRODUCTION

The difference between the transition energy of a dye molecule in a solvent and that in the gas phase is known as the solvatochromic shift. This shift reflects the interaction between the dye molecule (solute) and its solvent environment. Understanding the mechanism of solvatochromic shift is important in studies of spectroscopy and in practical applications of dyes. Several studies have been conducted on the mechanisms of solvatochromic shifts based on quantum-mechanical treatments, and many models have been proposed.[1−5] Several models show that the general hypsochromic shift (red shift) for $\pi-\pi^*$ transitions is proportional to the square of the transition dipole moments, which is sometimes regarded as the solvation energy of the transition dipole.[6] However, predictions by such models occasionally deviate from observations. Recently, Renger et al. proposed a new spectroscopic rule for solvatochromic shifts in nonpolar solvents based on the quantum-mechanical perturbation theory. This rule states that "the higher the excited state of the solute, the larger the solvatochromic shift," and the shift does not depend on the oscillator strength of the transition.[7]

In the present study, we examined mechanisms of the solvent effect on $\pi-\pi^*$ excitations of free-base porphine (FBP). Solvent effects on the ultraviolet−visible (UV−vis) absorption spectra of porphyrins have been studied extensively. For FBP, two Q-bands (the Q_x- and Q_y-bands) are observed in the visible region, and a strong B-band (Soret band) is observed in the UV region. Comparing the vapor-phase spectrum with that in solution, although temperature effects must be considered for the vapor phase experiment, one can see a bathochromic shift for the B-band and a decrease of the splitting width between the Q_x- and Q_y-bands caused by solvation.[8]

FBP does not have a permanent dipole moment, and therefore, the solute−solvent interactions can be explained in terms of dispersive forces. Renge studied the solvatochromic behavior of several tetrapyrrole pigments for many solvents.[9] Excellent linear dependence of the absorption energies on the Lorentz−Lorenz function was observed in *n*-alkanes for the Q- and B-bands. This predominating shift, which depends on the solvent polarizability, is associated with the difference in dispersion forces between the solvent and solute in the ground and the excited states. For free-base compounds, the Q-band energies were significantly affected by dipolar and quadrupolar solvents. The decrease in the Q-band splitting was supposed to be the effect of solvents on the molecular geometry: the dielectric properties of the solvent may modulate the mutual distance of central hydrogens.[10]

Quantum chemical computations have been performed for the understanding of the solvatochromism of porphyrins.

Received: May 30, 2012

   dx.doi.org/10.1021/ct300439r | J. Chem. Theory Comput. XXXX, XXX, XXX−XXX

Improta et al. reported the time-dependent (TD) density functional theory (DFT) calculations on the absorption spectra of porphyrins by considering solvent effects using the polarizable continuum model (PCM). Their TDDFT/PCM calculations reproduced the observed solvent effects on FBP with good accuracy.[11] As a more realistic model beyond PCM, quantum mechanics/molecular mechanics (QM/MM) simulations have been performed. Kowalski et al. reported on QM/MM calculations using a long-range corrected TDDFT[12] and the equation of motion-coupled cluster (EOM-CC) method[13] for the excited states of zinc porphyrin in aqueous solution. Their results showed a significant solvatochromic shift for N-band states that had a strong charge-transfer (CT) character, whereas the shift for the Q- and B-bands was negligible. These findings using the QM/MM disagree with the TDDFT/PCM results.

The origin of solute−solvent interactions described by continuum approximations has been discussed for electronic excitations. Cammi et al. studied models of solvatochromic shifts in terms of state-specific (SS) and linear-response (LR) treatments for solute−solvent interactions.[14] They showed that the SS and LR models involve different interaction terms. The LR treatment does not consider a relaxation of the electronic states of the solvent induced by the excitation of solute. The discrepancy between the SS and LR treatments was studied by Corni et al. in detail.[15] Their analysis based on the simplest four-state model showed that the solvatochromic shift in the LR method was proportional to the square of the transition moment, but such a contribution does not appear in the SS method. The term that includes the square of the transition moment is derived from entanglement terms in a many-body theory, and this term may not appear in a continuum-like approximation, in which a dynamical correlation between the solute and the solvent is not considered. Therefore, the SS and LR methods may provide different results for the same system. Indeed, we recently found that the solvatochromic behaviors for the $\pi-\pi^*$ excitations of bis-thienyl-ethenyl-benzene dyes calculated using SS and LR PCMs were different.[16] For nonpolar systems, the entanglement terms that include dispersive interactions are important, but these terms are entirely absent from the SS PCM.

In this study, we investigated the mechanism of solvent effects on the absorption spectra of FBP using quantum-chemical calculations and several solvation models. We adopted dichloromethane (CH_2Cl_2) and benzene (C_6H_6) as representative weakly polar and nonpolar solvents, respectively. The solvent effects on the excitation energies of the Q- and B-band states were examined. The excitation energies were calculated using the TDDFT and the symmetry-adapted cluster-configuration interaction (SAC-CI) method in PCM.[17,18] The LR and SS schemes of PCM were compared for the TDDFT calculations. We found that the SS scheme did not reproduce the experimental findings, whereas the LR scheme reproduced the experimental shifts. The effects from explicit solvent molecules were examined, and it was found that specific solute−solvent interactions are important for the Q-band splitting. We also considered QM/MM calculations and found that QM/MM with fixed MM charges are not appropriate for $\pi-\pi^*$ excitations of porphyrins. The dispersive interactions between the solute and solvent are the dominant origin of the solvatochromic shifts of FBP. In dipolar and quadrupolar solvents, specific interactions affect the Q-band splitting, although such effects can be partly described by the PCM. On the basis of the Casimir−Polder formula and a decomposition analysis, we found that the dominant part of the solute−solvent interactions can be considered using independent particle approximations, such as the configuration interaction with single excitations (CIS).

2. THEORETICAL BACKGROUND

2.1. Linear-Response and State-Specific Schemes for the PCM. The formal differences between the LR and SS schemes for the PCM have been discussed in detail by Cammi and co-workers.[14,15] Therefore, we provide here only an outline of these schemes. For simplicity, the nonequilibrium solvation effect is omitted from the discussion in this section. In the PCM, the solvent effect is described by solving a nonlinear Schrödinger equation for solute M:

$$H_M(\Psi_i)|\Psi_i\rangle = E_i|\Psi_i\rangle \tag{1}$$

with

$$H_M(\Psi_i) = H_M^{\mathrm{vac}} + V(\Psi_i) \tag{2}$$

where H_M^{vac} is the Hamiltonian of the isolated solute and V is a nonlinear operator that describes the interaction of the solute with the solvent. This may be written in the form

$$V(\Psi_i) = A\langle\Psi_i|B|\Psi_i\rangle \tag{3}$$

The Hamiltonian in eq 2 depends on the ith electronic state $|\Psi_i\rangle$ specifically, and thus, this scheme is termed the "state-specific" approach for solvation. Because of its nonlinearity, eq 1 must be solved iteratively in a self-consistent manner. The free-energy of the system can be written as

$$G(\Psi_i) = \langle\Psi_i|H_M(\Psi_i)|\Psi_i\rangle - \frac{1}{2}\langle\Psi_i|V(\Psi_i)|\Psi_i\rangle \tag{4}$$

and the transition energy for the $0 \rightarrow i$ excitation is defined as

$$\Delta G_{0i} = G(\Psi_i) - G(\Psi_0) \tag{5}$$

Using the perturbation expansion and correcting the first order terms, the transition energy up to the first order is given by

$$\Delta G_{0i}^{I} = \Delta E_{0i}^{(0)} + \frac{1}{2}[\langle\Psi_i^{(0)}|A|\Psi_i^{(0)}\rangle - \langle\Psi_0|A|\Psi_0\rangle] [\langle\Psi_i^{(0)}|B|\Psi_i^{(0)}\rangle - \langle\Psi_0|B|\Psi_0\rangle] \tag{6}$$

where $\Delta E_{0i}^{(0)} = E_i^{(0)} - E_0^{(0)}$ denotes the transition energy in a vacuum.

Another approach for calculating excitation energies is the linear-response theory, in which excitation energies are obtained as poles, ω_i, of the linear response amplitude of the TD Schrödinger equation for a solute in the ground state. This results in an eigenvalue problem with the form

$$\mathbf{G}\beta_i = \omega_i\mathbf{S}\beta_i \tag{7}$$

where $\mathbf{G}$ denotes the free-energy matrix and $\mathbf{S}$, the overlap matrix. Using the perturbation expansion, the excitation energy of the LR theory up to the first order is given by

$$\omega_i^{I} = \Delta E_{0i}^{(0)} + \langle\Psi_i^{(0)}|A|\Psi_0\rangle\langle\Psi_0|B|\Psi_i^{(0)}\rangle \tag{8}$$

where the zeroth-order wave function is obtained by

$$H_M(\Psi_0)|\Psi_i^{(0)}\rangle = E_i|\Psi_i^{(0)}\rangle \tag{9}$$

If we consider a simple dipole−dipole interaction, then these have the form

dx.doi.org/10.1021/ct300439r | J. Chem. Theory Comput. XXXX, XXX, XXX−XXX

$$\Delta G_{0i}^{I} = \Delta E_{0i}^{(0)} - \frac{1}{2}(\mu_{ii} - \mu_{00})g(\mu_{ii} - \mu_{00}) \tag{10}$$

and

$$\omega_i^{I} = \Delta E_{0i}^{(0)} - \mu_{i0}g\mu_{0i} \tag{11}$$

where μ is the dipole operator and g is the reaction field factor with $\mu_{ij} = \langle\Psi_i|\mu|\Psi_j\rangle$. The SS and LR methods contain different terms of interaction as their dominant (lowest-order) contributions. The PCM does not consider the explicit many-body interactions between the solute and solvent. Such interactions should be considered using the many-body perturbation theory described next.

2.2. Perturbation Theory for Solute−Solvent Dispersive Interactions. In this section, we will show the origin of the term including the square of the transition dipole moments that appears in the interaction energy by the perturbation theory. The perturbation theory for solute−solvent interaction was first reported by Ooshika.[1] Here, we start from a simpler formula given by Longuet-Higgins and Pople, in which the interaction between a solute and a single solvent molecule is considered.[2] A more general treatment was also given by McRae.[3] The zeroth-order equation for the solute may be given as

$$H_0|\psi_m\rangle = E_m|\psi_m\rangle \tag{12}$$

and for the solvent as

$$H_0|\varphi_M\rangle = E_M|\varphi_M\rangle \tag{13}$$

Here, the energies are shifted as the ground state of the solvent is zero. The wave function of the total system is expanded by the Hartree product of the solute and solvent wave functions:

$$\Psi_j = \sum_{Mm} \psi_m\varphi_M c_{mM}^{j} \tag{14}$$

The overlap between solute and solvent wave functions can be ignored for well-separated molecules. An interaction operator V can be written in separately as

$$\begin{aligned}(\psi_i\varphi_M|V|\psi_j\varphi_N) &= (\psi_i|A|\psi_j)(\varphi_M|B|\varphi_N)\\ &= A_{ij}B_{MN}\end{aligned} \tag{15}$$

For a simple dipole−dipole interaction, this term becomes

$$A_{ij}B_{MN} = (\psi_i|\mu|\psi_j)\cdot\left(\varphi_M\left|\frac{\mu}{r^3}\right|\varphi_N\right) \tag{16}$$

For nonpolar solute and solvent, the contributions that contain μ_{ii} and μ_{KK} are zero; therefore, the interaction energy for the solute in the ith state and the solvent in the ground state may be given by the second-order perturbation theory as

$$\Delta E_{i0}^{(2)} = -\sum_{j\neq i}\sum_{K>0}\frac{A_{ij}A_{ji}B_{0K}B_{K0}}{(E_j - E_i) + E_K} \tag{17}$$

This describes the interaction between nonpolar solute and nonpolar solvent, and we call such terms the dispersive interaction.

Several approximations have been used to reduce the energy denominator of eq 17, but different approximations lead to different conclusions.[1−5,7] Here, we use the Casimir−Polder formula[19] for the solute−solvent interaction. For the ground state, the interaction energy $\Delta E_{00}^{(2)}$ is obtained from eq 17 with $i = 0$. Using the integral transformation

$$\frac{1}{x+y} = \frac{2}{\pi}\int_0^\infty d\omega \frac{x}{x^2+\omega^2}\frac{y}{y^2+\omega^2} \tag{18}$$

which holds for $x, y > 0$, we obtain

$$\begin{aligned}\Delta E_{00}^{(2)} = -\frac{1}{2\pi}\int_0^\infty d\omega \sum_{j>0}\Bigg[&\frac{A_{0j}A_{j0}}{(E_j - E_0) + i\omega}\\ &+ \frac{A_{0j}A_{j0}}{(E_j - E_0) - i\omega}\Bigg]\sum_{K>0}\left[\frac{B_{0K}B_{K0}}{E_K + i\omega} + \frac{B_{0K}B_{K0}}{E_K - i\omega}\right]\end{aligned} \tag{19}$$

This can then be written as

$$\Delta E_{00}^{(2)} = -\frac{1}{2\pi}\int_0^\infty d\omega\ \alpha_g(i\omega)g_e(i\omega) \tag{20}$$

where

$$\alpha_g(i\omega) = -\sum_{j>0}\left[\frac{A_{0j}A_{j0}}{(E_j - E_0) + i\omega} + \frac{A_{0j}A_{j0}}{(E_j - E_0) - i\omega}\right] \tag{21}$$

and

$$g_e(i\omega) = \sum_{K>0}\left[\frac{B_{0K}B_{K0}}{E_K + i\omega} + \frac{B_{0K}B_{K0}}{E_K - i\omega}\right] \tag{22}$$

If a dipolar interaction, $A = \mu$, is considered, then eq 21 coincides with the dipole polarizability of the solute in the ground state with an imaginary frequency.

For the ith excited state, the interaction is given by eq 17. Because $E_j - E_i$ is not always positive, the integral transformation cannot be applied in this form for excited states, and thus, we rewrite eq 17 as

$$\begin{aligned}\Delta E_{i0}^{(2)} = &-\sum_{j>i}\sum_{K>0}\frac{A_{ij}A_{ji}B_{0K}B_{K0}}{(E_j - E_i) + E_K}\\ &+\sum_{j<i}\sum_{K>0}\frac{A_{ij}A_{ji}B_{0K}B_{K0}}{-(E_j - E_i) + E_K}\\ &-\sum_{j<i}\sum_{K>0}\frac{A_{ij}A_{ji}B_{0K}B_{K0}}{(E_j - E_i) + E_K}\\ &-\sum_{j<i}\sum_{K>0}\frac{A_{ij}A_{ji}B_{0K}B_{K0}}{-(E_j - E_i) + E_K}\end{aligned} \tag{23}$$

Here, we assume that the states are arranged in order of increasing energy, and thus, the summation over $j < i$ applies for $E_j < E_i$. Then, the integral transformation can be applied to the first and second terms, and we obtain

$$\begin{aligned}\Delta E_{i0}^{(2)} = &-\frac{1}{2\pi}\int_0^\infty d\omega \sum_{j\neq i}\frac{2(E_j - E_i)A_{ij}A_{ji}}{(E_j - E_i)^2 + \omega^2}\\ &\sum_{K>0}\frac{2E_K B_{0K}B_{K0}}{E_K^2 + \omega^2} - \sum_{j<i}A_{ij}A_{ji}\\ &\sum_{K>0}\left[\frac{B_{0K}B_{K0}}{E_K + (E_j - E_i)} - \frac{B_{0K}B_{K0}}{E_K - (E_j - E_i)}\right]\end{aligned} \tag{24}$$

dx.doi.org/10.1021/ct300439r | J. Chem. Theory Comput. XXXX, XXX, XXX−XXX

This can be written as

$$\Delta E_{i0}^{(2)} = -\frac{1}{2\pi}\int_0^\infty d\omega\ \alpha_i(i\omega) g_e(i\omega) - \sum_{j<i} A_{ij}A_{ji}g(\nu_{ji}) \tag{25}$$

where

$$\alpha_i(i\omega) = -\sum_{j\neq i}\left[\frac{A_{ij}A_{ji}}{(E_j - E_i) + i\omega} + \frac{A_{ij}A_{ji}}{(E_j - E_i) - i\omega}\right] \tag{26}$$

and

$$g(\nu_{ji}) = \sum_{K>0}\left[\frac{B_{0K}B_{K0}}{E_K + \nu_{ji}} - \frac{B_{0K}B_{K0}}{E_K - \nu_{ji}}\right] \tag{27}$$

with

$$\nu_{ji} = E_j - E_i \tag{28}$$

If dipolar interactions are considered, then eq 26 can be considered as describing the dipole polarizability of the solute in the ith state with an imaginary frequency.

The solvatochromic shift is given by

$$\Delta E_{i0}^{(2)} - \Delta E_{00}^{(2)} = -\frac{1}{2\pi}\int_0^\infty d\omega\ g_e(i\omega)[\alpha_i(i\omega) - \alpha_g(i\omega)] - \sum_{j<i} A_{ij}A_{ji}g(\nu_{ji}) \tag{29}$$

This is a generalization of the formula given by Corni et al.[15] for many states. An important feature of our formulation is the derivation of the de-excitation terms. The right-hand side of eq 27 may be written as

$$\frac{B_{0K}B_{K0}}{E_K + \nu_{ji}} - \frac{B_{0K}B_{K0}}{E_K - \nu_{ji}} = -2\frac{B_{0K}B_{K0}}{E_K}\frac{\nu_{ji}/E_K}{1 - (\nu_{ji}/E_K)^2} \tag{30}$$

If $\nu_{ji} \ll E_K$, then eq 27 is proportional to ν_{ji}, and ν_{0i} provides the largest contribution. If we take only ν_{0i} and consider $A = \mu$, then the solvatochromic shift may be written as

$$\Delta E_{i0}^{(2)} - \Delta E_{00}^{(2)} \approx -\frac{1}{2\pi}\int_0^\infty d\omega\ g_e(i\omega)[\alpha_i(i\omega) - \alpha_g(i\omega)] - \mu_{0i}^2 g(\nu_{0i}) \tag{31}$$

The first contribution represents the difference in polarizability between the ground and excited states. The second term represents the interaction between the transition dipole and the reaction field generated by the polarizable solvent. A similar result was obtained by Basu.[4] The transition dipole appears as the complement of the de-excitation terms in the expression of the polarizability in the excited state. $g(\nu_{ji})$ is always positive because $\nu_{ji} < 0$ and $E_K > \nu_{ji}$ hold; therefore, the second term on the right-hand side of eq 29 always gives the bathochromic shift for states with a nonzero intensity.

3. COMPUTATIONAL DETAILS

We used the following four models to investigate the electronic origin of the solvent effects on the electronic excitation energies of FBP:

(1) conventional quantum mechanical calculations for FBP in a vacuum, which were a reference for the solvatochromic shifts
(2) the PCM, in which solvent circumstances were modeled using a polarizable continuum and FBP was treated using quantum mechanical calculations
(3) the explicit solvation model, in which FBP and several solvent molecules were treated using quantum mechanical calculations
(4) the PCM combined with an explicit solvation model, in which FBP and explicit solvent molecules were embedded in a polarizable continuum

All of the computations were performed using the Gaussian 09 software package and its development versions.[20] The molecular geometries were optimized using the B3LYP method[21] and the 6-31G** basis set[22] in a vacuum. The effect of the geometry relaxation in solution may be a source of solvatochromic shifts, but such an effect would be minor for FBP because the molecular framework is rigid (see the Supporting Information). Therefore, we ignored the effect of geometry relaxation in solution in our computations.

For the explicit solvation model, individually optimized solute and solvent molecules were oriented and the intermolecular distances were optimized without considering the relaxation of the internal molecular geometries. The basis set superposition error (BSSE) correction was considered for single point calculations, but the correction was omitted for the optimization of the intermolecular distances. The dispersion interaction was significant for the present systems, and we therefore used the wB97XD functional,[23] which includes empirical dispersion interactions. The intermolecular distances obtained using wB97XD were almost identical to those obtained with the second-order Møller–Plesset perturbation theory (MP2) calculations. Conformations that could preserve D_{2h} point group symmetry were used as the simplest explicit solvation model because we intended to focus on the effects of electronic interactions, so it was necessary to exclude the effects from the geometry relaxation. Two models were used for the explicit solvation calculations. The first was a π-interaction model, in which two solvent molecules were placed on both sides of the molecular plane of FBP. The second was a σ-interaction model, in which four solvent molecules were oriented on the edges of FBP.

For the π-interaction model of FBP–$(CH_2Cl_2)_2$, the orientation shown in Figure 1 was found to be the most stable within the D_{2h} symmetry. The CH bonds of CH_2Cl_2 are

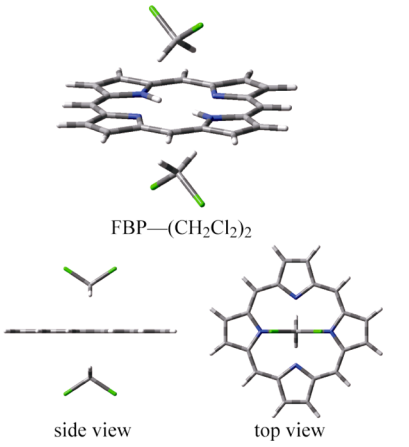

Figure 1. A projection figure, side view, and top view of the FBP–$(CH_2Cl_2)_2$, π-interaction model system.

dx.doi.org/10.1021/ct300439r | J. Chem. Theory Comput. XXXX, XXX, XXX–XXX

oriented toward the unprotonated nitrogen atom of FBP; the interaction energy between the unprotonated nitrogen and methylene was larger than that between the pyrrole proton and chlorine. The distance between the center of the FBP molecule and the carbon atom of CH_2Cl_2 was 2.70 Å. The interaction energy of the entire system was 17.2 kcal/mol using the wB97XD/6-31G** method including a counterpoise (CP) correction for the BSSE. For the σ-interaction model, the orientation shown in Figure 2, in which the CH bonds of

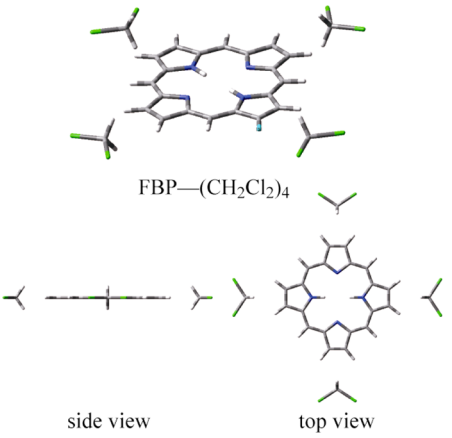

Figure 2. A projection figure, side view, and top view of the FBP–$(CH_2Cl_2)_4$, σ-interaction model system.

CH_2Cl_2 are oriented toward the FBP molecule, was stable. The distance between the center of the FBP molecule and the carbon atom of CH_2Cl_2 was 7.60 Å for all CH_2Cl_2 molecules. In this geometry, the distance between the peripheral C–C bonds of the FBP molecule and the carbon atom of CH_2Cl_2 was about 3.34 Å. The interaction energy of the entire system was 5.6 kcal/mol (with a CP correction).

For the π-interaction model of FBP–$(C_6H_6)_2$, the orientation shown in Figure 3 was found to be the most stable within the D_{2h} symmetry. The interplane distance between the FBP and C_6H_6 molecules was 3.10 Å. The interaction energy of the entire system was 13.2 kcal/mol using the wB97XD/6-31G** method with a CP correction. For the σ-interaction

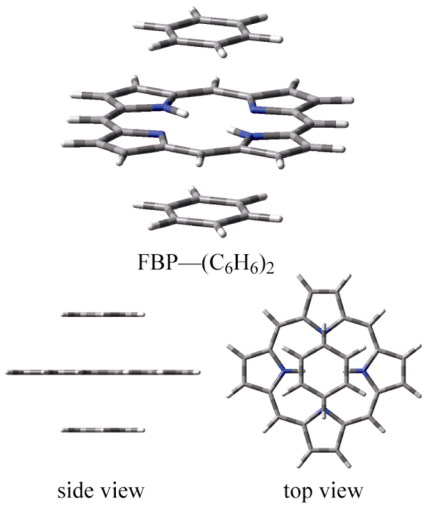

Figure 3. A projection figure, side view, and top view of the FBP–$(C_6H_6)_2$, π-interaction model system.

model, the orientation shown in Figure 4, in which C_6H_6 molecules are oriented along the meso-positions of FBP, was

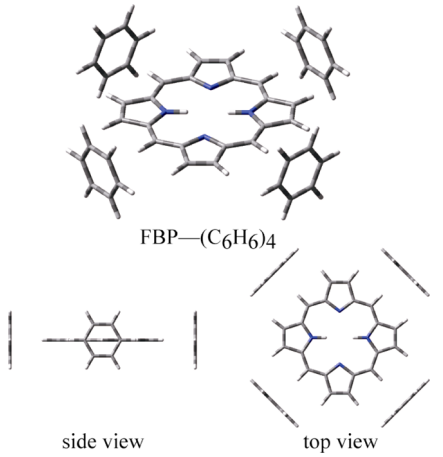

Figure 4. A projection figure, side view, and top view of the FBP–$(C_6H_6)_4$, σ-interaction model system.

stable. The distance between the meso carbon atom of the FBP molecule and the center of the C_6H_6 molecule was 3.66 Å. The interaction energy of the entire system was 18.2 kcal/mol (with a CP correction). The interaction energy would result from the CH/π interaction.

The electronic excitation energies were calculated using the TDDFT and SAC-CI methods with the D95(d) basis set.[24] For the TDDFT calculations, we employed the B3LYP, PBE0 (PBE1PBE),[25] and CAM-B3LYP[26] functionals. For the TDDFT and SAC-CI calculations, the core orbitals that corresponded to the 1s electrons of the C, N, and Cl atoms and 2s2p electrons of the Cl atoms and the complementary virtual orbitals were excluded as frozen-core approximations. The perturbation selection technique was used for the SAC and SAC-CI calculations. The double excitation operators having second-order contributions to the energy that were less than the given threshold were excluded from the calculations. The thresholds for the perturbation selection were 1.0×10^{-7} and 1.0×10^{-8} for the ground and excited states, respectively. The accuracy of the perturbation selection for the PCM SAC/SAC-CI calculations was tested using several thresholds, and we confirmed that the present thresholds were sufficiently accurate (see the Supporting Information). The GSUM method was used to calculate explicit solvation models to ensure a smooth potential energy surface within the selected operator space.[27] We took the sum of selected operators between the calculated intermolecular distances and those of widely separated distances. The SAC-CI calculations were performed using the latest direct SAC-CI program[28] combined with the PCM.[17,18]

The integral equation formula (IEF)-PCM[29] with the default parameters in Gaussian 09 were used in all of the PCM calculations. The nonequilibrium solvation was considered for vertical excitations in the PCM.[18,30−32] For TDDFT calculations with the PCM, we examined the LR and SS solvation schemes. For the SS calculations, the external iteration procedure for each excited state is necessary to obtain a self-consistent solution of nonlinear equations. For the LR calculations, no iteration procedure is necessary for excited states.[33] For SAC-CI calculations with the PCM, only the SS solvation scheme has been implemented, and so we examined the SS solvation in the SAC-CI calculations. The PCM SAC/

dx.doi.org/10.1021/ct300439r | J. Chem. Theory Comput. XXXX, XXX, XXX–XXX

SAC-CI program has been implemented in the GAUSSIAN development version. This study discusses singlet states only; therefore, the notations of spin state are omitted. The static polarizabilities were calculated using the numerical differentiation of the dipole moment with respect to an external electronic field; the dipole moments of the ground and excited states were obtained from the analytical energy derivative of the DFT and TDDFT, respectively.

4. RESULTS AND DISCUSSION

4.1. Solvatochromic Shifts with the PCM. Table 1 shows the calculated excitation energies of FBP in a vacuum and their solvatochromic shifts from PCM calculations. In a vacuum, the results from the B3LYP and PBE0 functionals are very close, although the PBE0 functional gives slightly higher excitation energies. The long-range correction included in the CAM-B3LYP method reduces the excitation energies of the Q-band $1B_{3u}$ and $1B_{2u}$ states, and the correction increases the excitation energies of the B-band $2B_{3u}$ and $2B_{2u}$ states by about 0.2 eV compared with the B3LYP results. The SAC-CI calculations further reduce the excitation energy of the Q_x-band ($1B_{3u}$ state) and increase the energy of the B-band. The difference between the SAC-CI and TDDFT methods for porphyrins has been discussed previously.[35]

Table 1. Excitation Energies (EE), Oscillator Strengths (Osc), and Solvatochromic Shifts in PCM Calculations[a]

	in vacuum	in CH_2Cl_2		in C_6H_6	
state	EE (Osc)	LR PCM	SS PCM	LR PCM	SS PCM
		B3LYP			
$1B_{3u}$	2.268 (0.000)	+0.012	+0.031	+0.003	+0.013
$1B_{2u}$	2.422 (0.000)	+0.003	+0.021	−0.004	+0.009
$2B_{3u}$	3.322 (0.444)	−0.087	+0.062	−0.124	+0.021
$2B_{2u}$	3.484 (0.662)	−0.150	+0.055	−0.189	+0.017
		CAM-B3LYP			
$1B_{3u}$	2.173 (0.002)	+0.012	+0.034	+0.001	+0.015
$1B_{2u}$	2.393 (0.001)	−0.005	+0.013	−0.011	+0.005
$2B_{3u}$	3.533 (0.843)	−0.151	+0.067	−0.192	+0.027
$2B_{2u}$	3.660 (1.183)	−0.208	+0.043	−0.249	+0.018
		PBE0			
$1B_{3u}$	2.303 (0.001)	+0.014	+0.034	+0.003	+0.014
$1B_{2u}$	2.466 (0.001)	+0.003	+0.022	−0.005	+0.005
$2B_{3u}$	3.402 (0.543)	−0.104	+0.066	−0.144	+0.028
$2B_{2u}$	3.561 (0.871)	−0.174	+0.056	−0.214	+0.018
		SAC-CI			
$1B_{3u}$	1.903 (0.004)		+0.030		+0.012
$1B_{2u}$	2.376 (0.004)		+0.003		−0.001
$2B_{3u}$	3.638 (1.418)		+0.041		+0.016
$2B_{2u}$	3.776 (2.026)		+0.031		+0.013

experiment	EE	Shift in CH_2Cl_2	Shift in C_6H_6
Q_x	1.976[b], 2.023[c]	−0.002[d]	−0.015[d]
Q_y	2.424[b], 2.465[c]	−0.071[d]	−0.084[d]
B	3.328[b]	−0.177[e]	−0.201[e]

[a]The energies are given in eV. [b]Vapor phase spectrum (393 °C) from ref 8. [c]The 0−0 transition in supersonic expansion of helium from ref 34. [d]From ref 8 and the shift from supersonic experiment. [e]From ref 8 and the shift from vapor phase spectrum.

With the LR PCM, the Q-band shifts were calculated around 0.01 eV or less, while the calculated shifts of B-bands (second states) were significant, being 0.1−0.2 eV and bathochromic. The shifts in C_6H_6 were 1.2−1.4 times larger than those in CH_2Cl_2. This can be explained by the nonequilibrium effect.

In the nonequilibrium solvation scheme, the solvent polarization vector, **P**, is divided into fast (or dynamical) and slow (or inertial) components as

$$\mathbf{P} = \mathbf{P}_{dyn} + \mathbf{P}_{in} \tag{32}$$

The total polarization **P** and dynamical polarization $\mathbf{P}_{dyn}$ are determined by the static dielectric constant ε_0 and the optical dielectric constant ε_∞ of the solvent, respectively. The optical dielectric constant is related to the refractive index, n, of the bulk solvent as $\varepsilon_\infty = n^2$. The dielectric constants of CH_2Cl_2 used for the PCM were $\varepsilon_0 = 8.93$ and $\varepsilon_\infty = 2.028$, and those for C_6H_6 were $\varepsilon_0 = 2.271$ and $\varepsilon_\infty = 2.253$. For the vertical excitation energies, the effect from the dynamical polarization was significant in the LR PCM calculation. This dependence of the calculated shifts on ε_∞ agrees with the observed linear dependence of the absorption energies[9] on the Lorentz−Lorenz function $\phi(n^2) = (n^2 - 1)/(n^2 + 2)$. The order of the solvatochromic shift for the B-band states was B3LYP < PBE0 < CAM-B3LYP. This order corresponds to both the intensity of the transition and the magnitude of the transition dipole moments. This observation agrees with the finding that the shift in the LR PCM calculations was dependent on the transition moment in eq 11.

In the SS PCM calculations, the obtained solvatochromic shifts showed significantly different trends from the LR PCM results. The calculated solvatochromic shifts were positive for almost all states in both CH_2Cl_2 and C_6H_6. The magnitude of the shift was around 0.02−0.07 eV. The shift for the B_{3u} states was larger than that for the B_{2u} states. The shift in C_6H_6 was about 30−40% of that in CH_2Cl_2. The trend in shifts obtained using the TDDFTs was basically the same as that in the SAC-CI calculations, although for the $1B_{2u}$ state, the shift in the SAC-CI was rather small. The effect from $\mathbf{P}_{in}$ increased during the self-consistent process considered in the SS PCM calculation. The leading-order effect considered by the SS PCM calculation is the difference in the dipole moments of the ground and excited states as shown by eq 10. FBP does not have a permanent dipole moment, and therefore, the leading-order contribution to the shift is zero. Then, the calculated shifts originate in the higher-order effects.

The experimental absorption spectra in the vapor phase and in solution were reported in ref 8; from the reported band maxima, the Q_x and Q_y-bands showed bathochromic and hypsochromic solvent shifts, respectively. However, a thermal bathochromic effect is probably involved in the vapor-phase spectrum of ref 8. Therefore, we used the 0−0 transition energies measured in the supersonic expansion of helium[34] for the standard of solvatochromic shift of Q-bands. The shift value for the Q_x-band is smaller than that for the Q_y-band; thus, the width of the split between the Q_x- and Q_y-bands decreases in solution.

The experimentally observed trends in the solvatochromic shifts were reproduced by the LR PCM calculations: the decrease in the energy difference between the Q_x- and Q_y-bands and the bathochromic shift of the B-band. The LR PCM calculations could also explain the larger shift for the B-band in C_6H_6 than that in CH_2Cl_2 because C_6H_6 has a larger optical dielectric constant than CH_2Cl_2. The SS PCM calculation could describe the decrease in the energy difference between the Q_x- and Q_y-bands, whereas it failed to reproduce the bathochromic shift of the B-band. The calculated hypsochromic shifts by the

dx.doi.org/10.1021/ct300439r | J. Chem. Theory Comput. XXXX, XXX, XXX−XXX

SS PCM scheme may be artifacts. These shifts may result from a multipolar effect of the solvent reaction field considered during the self-consistent iterations. Benzene can be considered to be a pseudopolar solvent because of its large quadrupole moment. The hypsochromic shifts would be corrected by the dispersive interaction.

4.2. Solvatochromic Shifts from Explicit Solvent Molecules. Table 2 shows the calculated solvatochromic shifts

Table 2. Solvatochromic Shifts (in eV) for Explicit Solvent Molecules

state	$(CH_2Cl_2)_2$	$(CH_2Cl_2)_4$	$(C_6H_6)_2$	$(C_6H_6)_4$
		B3LYP		
$1B_{3u}$	+0.016	−0.009	−0.025	−0.012
$1B_{2u}$	−0.005	−0.009	−0.024	−0.012
$2B_{3u}$	+0.025	+0.001	−0.110	−0.010
$2B_{2u}$	−0.027	−0.006	−0.133	−0.030
		CAM-B3LYP		
$1B_{3u}$	+0.014	−0.008	−0.018	−0.008
$1B_{2u}$	−0.013	−0.008	−0.018	−0.010
$2B_{3u}$	−0.001	−0.015	−0.142	−0.031
$2B_{2u}$	−0.051	−0.026	−0.158	−0.050
		SAC-CI		
$1B_{3u}$	+0.020	−0.009	−0.022	−0.010
$1B_{2u}$	−0.033	−0.011	−0.031	−0.017
$2B_{3u}$	−0.017	−0.019	−0.170	−0.042
$2B_{2u}$	−0.066	−0.027	−0.180	−0.054

using explicit solvent molecules. The results with the PBE0 and B3LYP functionals showed similar trends (Supporting Information). In CH_2Cl_2, the solvent shifts in the σ-interaction model $(CH_2Cl_2)_4$ were negative except for the $2B_{3u}$ state with B3LYP. The shifts described by the B3LYP were relatively small, less than 0.01 eV. The shifts of the B-bands increased using the CAM-B3LYP and SAC-CI methods, because of the long-range exchange interactions involved.

The solvent shifts in the π-interaction model $(CH_2Cl_2)_2$ were more significant than those in the σ-interaction model. With the B3LYP calculation, the shift was positive for the B_{3u} states and negative for the B_{2u} states, whereas the shift for the $2B_{2u}$ state was negative with the CAM-B3LYP and SAC-CI. Thus, the solvent shifts of the B_{2u} and B_{3u} states were in opposite directions. This trend may be explained by the asymmetric interaction between CH_2Cl_2 molecules and FBP; i.e., the interaction between the hydrogen atoms of CH_2Cl_2 and the lone pair of FBP nitrogen atoms. This behavior reduces the energy difference between the B_{3u} and B_{2u} states, and consequently, the splitting between the Q_x- and Q_y-bands becomes small. In addition, the long-range exchange interactions may be important for the B-band. The SAC-CI and CAM-B3LYP calculations could reproduce the bathochromic shift of the B-band in the $(CH_2Cl_2)_2$ model calculations, although the magnitude of the shift was underestimated by this simplest model.

In C_6H_6, the solvent shifts from the σ-interaction model $(C_6H_6)_4$ were negative, and the degree of the shift was 0.01−0.05 eV. The solvent shifts from the π-interaction model $(C_6H_6)_2$ were significant, particularly for the B-bands. The shifts were negative for both the B_{3u} and B_{2u} states. The shift values of the $1B_{3u}$ and $1B_{2u}$ states were almost equal in the TDDFT results, while such equivalence was slightly broken in the SAC-CI results. The shifts of the $2B_{3u}$ and $2B_{2u}$ states were about 0.11−0.18 eV; the shift for the $2B_{2u}$ was larger than that for the $2B_{3u}$. The long-range exchange interaction increases the shift for the B-band. The SAC-CI method further enhanced the shift, probably because of the dispersive interactions considered.

From the SAC-CI calculations, the energy difference between the $1B_{2u}$ and $1B_{3u}$ states decreased in C_6H_6. This would indicate that the dispersion interaction between the solute and solvent decreases the energy difference. Indeed, the FBP−Ar van der Waals complex, in which dispersion interaction would be dominant, showed a similar decrease of the Q-band splitting.[36] The calculated decrease of the Q-band splitting in C_6H_6 is smaller than the observed values probably because the present solvation model is too restricted. As for CH_2Cl_2, anisotropic interaction with C_6H_6 molecules would enhance the energy difference between the $1B_{2u}$ and $1B_{3u}$ states.

4.3. Explicit Solvent Molecules in PCM. Table 3 shows the results for FBP with solvent molecules (the π-interaction

Table 3. Solvatochromic Shifts (in eV) of Explicit Solvent Molecules in the PCM

state	$(CH_2Cl_2)_2$ LR PCM	$(CH_2Cl_2)_2$ SS PCM	$(C_6H_6)_2$ LR PCM	$(C_6H_6)_2$ SS PCM
		CAM-B3LYP		
$1B_{3u}$	+0.016	+0.027	−0.020	−0.011
$1B_{2u}$	−0.018	+0.000	−0.029	−0.015
$2B_{3u}$	−0.140	+0.029	−0.265	−0.126
$2B_{2u}$	−0.213	−0.027	−0.303	−0.148

models) using the PCM and CAM-B3LYP method. The results with other methods are shown in the Supporting Information. The LR and SS PCM calculations still showed different trends in their shifts. In CH_2Cl_2, the trend in the LR PCM with $(CH_2Cl_2)_2$ results was similar to the trend in the LR PCM without explicit solvents for all states. The trend in the SS PCM with $(CH_2Cl_2)_2$ results was also similar to the trend in the SS PCM without explicit solvents, except for the $2B_{2u}$ state. This state was significantly affected by the explicit solvent molecules in the SS PCM calculations, and the shift became bathochromic.

In C_6H_6, the shifts from the PCM and the explicit solvents seemed to be approximately additive contributions. The bathochromic effects from the explicit $(C_6H_6)_2$ molecules and the LR PCM environment accumulated. On the other hand, the bathochromic effect from the explicit $(C_6H_6)_2$ and the hypsochromic effect from the SS PCM were canceled out. As a result, the LR PCM plus $(C_6H_6)_2$ model largely overestimated the solvatochromic shift in the B-band. Equations 10 and 11 state that the SS and LR PCM schemes provide the same results if $1/2(\mu_{ii} - \mu_{00})^2 = \mu_{0i}^2$ or $g = 0$ holds. The latter condition corresponds to the case in which the effect from the reaction field of a continuum is negligible, and so the PCM environment is not necessary. The former condition does not hold, at least for the present models, because the solute does not have a dipole moment even though the transition dipoles are nonzero.

4.4. Molecular Interactions in the Explicit Solvation Model. We further investigated the origin of solute−solvent interaction in solvatochromic shift using CIS wave functions, which is the simplest excited-state theory. The calculated solvatochromic shifts from the π-interaction model $(C_6H_6)_2$ with the CIS/D95(d) level of theory were −0.007, −0.007,

dx.doi.org/10.1021/ct300439r | J. Chem. Theory Comput. XXXX, XXX, XXX−XXX

−0.208, and −0.260 eV for the $1B_{3u}$, $1B_{2u}$, $2B_{3u}$, and $2B_{2u}$ states, respectively (see Table 4). The trends in the TDDFT and SAC-CI results were reproduced by the CIS calculations. Therefore, the dominant effect of the solute−solvent interaction can be discussed by analyzing the CIS wave functions.

Table 4. Energy Decomposition of CIS Solvatochromic Shifts for FBP−$(C_6H_6)_2$ in eV

	$1B_{3u}$	$1B_{2u}$	$2B_{3u}$	$2B_{2u}$
$\langle\Phi_M^M\|H\|\Phi_M^M\rangle$	+0.002	+0.002	−0.157	−0.203
$\langle\Phi_M^S\|H\|\Phi_M^S\rangle$	−0.007	−0.005	+0.000	−0.012
$\langle\Phi_S^M\|H\|\Phi_S^M\rangle$	+0.022	+0.022	+0.103	+0.127
$\langle\Phi_S^S\|H\|\Phi_S^S\rangle$	+0.002	+0.002	+0.257	+0.424
$\langle\Phi_M^M\|H\|\Phi_M^S\rangle$	+0.011	+0.008	+0.002	+0.021
$\langle\Phi_M^M\|H\|\Phi_S^M\rangle$	−0.034	−0.032	−0.087	−0.094
$\langle\Phi_M^M\|H\|\Phi_S^S\rangle$	−0.002	−0.003	−0.262	−0.418
$\langle\Phi_M^S\|H\|\Phi_S^M\rangle$	+0.000	+0.000	+0.000	+0.000
$\langle\Phi_M^S\|H\|\Phi_S^S\rangle$	+0.000	+0.000	−0.007	−0.013
$\langle\Phi_S^M\|H\|\Phi_S^S\rangle$	−0.001	−0.001	−0.056	−0.091
total shift	−0.007	−0.007	−0.208	−0.260

The excitation energy of the CIS (pth singlet state) can be written as

$$\Delta E_{\mathrm{CIS}}^{(p)} = \langle\Psi_{\mathrm{CIS}}^{(p)}|(H - E_{\mathrm{HF}})|\Psi_{\mathrm{CIS}}^{(p)}\rangle \tag{33}$$

where E_{HF} is the Hartree−Fock energy. The pth solution of the CIS wave function can be written as

$$\Psi_{\mathrm{CIS}}^{(p)} = \sum_{i}^{\mathrm{Occ}} \sum_{a}^{\mathrm{Vac}} C_{i\to a}^{(p)} |\Phi_i^a\rangle \tag{34}$$

and the wave function is normalized as $\langle\Psi_{\mathrm{CIS}}^{(p)}|\Psi_{\mathrm{CIS}}^{(p)}\rangle = 1$. Hereafter, i, j,... and a, b,... denote occupied and unoccupied (vacant) MOs, respectively. The singly excited configuration state functions are denoted by $|\Phi_i^a\rangle$. Using this, we obtain

$$\Delta E_{\mathrm{CIS}}^{(p)} = \sum_{ia}\sum_{jb} C_{i\to a}^{(p)} C_{j\to b}^{(p)} \langle\Phi_i^a|H|\Phi_j^b\rangle \tag{35}$$

If we use localized MOs, then all the MOs can be classified as solute (M) or solvent (S) MOs, namely,

$$\{i, j, ..., a, b, ...\} = \{i_M, j_M, ..., a_M, b_M, ...\} + \{i_S, j_S, ..., a_S, b_S, ...\} \tag{36}$$

Then, the Hamiltonian matrix elements will be denoted by

$$\langle\Phi_i^a|H|\Phi_j^b\rangle \rightarrow \begin{bmatrix} \langle\Phi_M^M|H|\Phi_M^M\rangle & \langle\Phi_M^M|H|\Phi_M^S\rangle & \langle\Phi_M^M|H|\Phi_S^M\rangle & \langle\Phi_M^M|H|\Phi_S^S\rangle \\ \langle\Phi_M^S|H|\Phi_M^M\rangle & \langle\Phi_M^S|H|\Phi_M^S\rangle & \langle\Phi_M^S|H|\Phi_S^M\rangle & \langle\Phi_M^S|H|\Phi_S^S\rangle \\ \langle\Phi_S^M|H|\Phi_M^M\rangle & \langle\Phi_S^M|H|\Phi_M^S\rangle & \langle\Phi_S^M|H|\Phi_S^M\rangle & \langle\Phi_S^M|H|\Phi_S^S\rangle \\ \langle\Phi_S^S|H|\Phi_M^M\rangle & \langle\Phi_S^S|H|\Phi_M^S\rangle & \langle\Phi_S^S|H|\Phi_S^M\rangle & \langle\Phi_S^S|H|\Phi_S^S\rangle \end{bmatrix} \tag{37}$$

The excitation energy and the solvatochromic shift can be decomposed into the terms shown in eq 37. The decomposed values of the solvatochromic shift are shown in Table 4, where the hermiticity of the matrix is considered. These values include a CP correction. Here, we calculated the excited states of the solute, and thus, the CP correction only works for the terms $\langle\Phi_M^M|H|\Phi_M^M\rangle$, $\langle\Phi_M^S|H|\Phi_M^S\rangle$, and $\langle\Phi_M^M|H|\Phi_M^S\rangle$ but was significant for these terms. Although the contribution of the BSSE was canceled out in the total values, the CP correction in each term was found to be very large. For other terms that include excitation from the solvent MO, the BSSE correction could not be estimated using the standard CP correction. Thus, the values of these terms in Table 4 may involve some component from the BSSE. These terms mainly represent the polarization of the solvent induced by the excitation of the solute.

Several significant terms for the $2B_{2u}$ and $2B_{3u}$ states are given in Table 4; these constitute the origin of the shift of the B-band. Here, we discuss the effect on the B-band states. The dominant part of the diagonal terms, such as $\langle\Phi_M^M|H|\Phi_M^M\rangle$ or $\langle\Phi_S^S|H|\Phi_S^S\rangle$, originates in the Fock matrix elements, i.e., the shift in the orbital energy owing to the solvation. The summation of the diagonal elements leads to a positive energy shift, and this type of interaction can be described using the SS PCM. A significant negative value appears in the off-diagonal $\langle\Phi_M^M|H|\Phi_S^S\rangle$ element. By further decomposition of this term, we found that the electron repulsion integrals with the form $(i_M a_M|j_S b_S)$ are dominant in the $\langle\Phi_M^M|H|\Phi_S^S\rangle$ element. Using the notation in eq 14, this matrix element may be written as

$$\langle\Phi_M^M|H|\Phi_S^S\rangle = \langle\psi_k\varphi_0|H|\psi_0\varphi_K\rangle \tag{38}$$

where ψ_k and φ_K denote the singly excited configurations of the solute and solvent, respectively. If we assume that the interaction operator can be written in the form shown in eq 15, then eq 38 may be rewritten as

$$\langle\Phi_M^M|H|\Phi_S^S\rangle = \langle\psi_k\varphi_0|AB|\psi_0\varphi_K\rangle \tag{39}$$

For the Hartree product of ψ_k and φ_K, we obtain

$$\langle\Phi_M^M|H|\Phi_S^S\rangle = \langle\psi_k|A|\psi_0\rangle\langle\varphi_0|B|\varphi_K\rangle \tag{40}$$

Therefore, this type of contribution is regarded as an entanglement term: a dynamical correlation term between the electrons in the solute and the solvent.[15] In the Brillouin condition, $\langle\psi_0|H|\psi_k\rangle = 0$ without solvent polarization, and therefore, the $\langle\Phi_M^M|H|\Phi_S^S\rangle$ term can be regarded as the correction of the Brillouin condition that arises from the solute−solvent interactions. The corresponding term appears in the LR PCM scheme in eq 11, although the SS PCM scheme does not contain such terms, probably because the Hamiltonian orthogonality is not imposed between the ground and excited states.

4.5. Effect of Solute Polarizability. The solute−solvent interactions are also regarded as interactions between induced dipole moments. In Onsager's theory,[37] the dipole moment of the solute may be written as

$$\mu_M = \mu_{\mathrm{p}} + \alpha_M \mathbf{F} \tag{41}$$

where μ_{p} is the permanent dipole moment of an isolate solute, α_M is its static polarizability, and $\mathbf{F}$ is a suitable reaction field. From this point of view, solvatochromic shifts may be related to the difference in polarizability between the ground and excited states, particularly for a solute without a permanent dipole moment. In such cases, polarization of the solvent environment must be considered for producing a field $\mathbf{F}$.

Table 5 shows the calculated polarizability using the DFT and TDDFT with the D95(d,p) basis set. By the calculations using the B3LYP and PBE0 functionals, the polarizabilities in the ground state (XA_g) and in the $1B_{3u}$ state had almost the same values. Using CAM-B3LYP, the polarizability in the $1B_{3u}$

dx.doi.org/10.1021/ct300439r | J. Chem. Theory Comput. XXXX, XXX, XXX−XXX

Table 5. Calculated Isotropic Static Polarizabilities (in Å^3)

state	B3LYP	CAM-B3LYP	PBE0
XA_g	49.10	48.47	48.96
$1B_{3u}$	49.19	47.59	48.92
$1B_{2u}$	51.71	51.14	51.58
$2B_{3u}$	107.52	56.09	83.68
$2B_{2u}$	96.87	52.11	67.28

state was smaller than that in the ground state, whereas the polarizability in the $1B_{2u}$ state was larger than that in the ground state. In this case, $\mu_p = 0$, and under the assumption that **F** is constant during electronic transitions, the $1B_{2u}$ state has a larger induced dipole than that in the ground state or $1B_{3u}$ state. Thus, the $1B_{2u}$ state will be stabilized by solvation and will show a bathochromic shift. The polarizability in the $2B_{3u}$ and $2B_{2u}$ states largely depends on the functionals. Even so, the polarizabilities of these states are larger than the ground state value. Renge has reported that the solvatochromic shifts of porphyrins can be explained by the polarizability changes between the ground and excited states. The estimated polarizability changes in refs 9 and 38 by experimental spectra are roughly consistent with our computations.

If we use the London approximation,[39] in which the dispersive interactions described by the dynamic polarizabilities with an imaginary frequency are replaced by static polarizabilities and ionization potentials, then the solvatochromic shift described by eq 31 can be written as

$$\Delta E_{i0}^{(2)} - \Delta E_{00}^{(2)} \approx -C_1(\alpha_i - \alpha_0) - \mu_{0i}^2 g \qquad (42)$$

where C_1 is a constant that depends on the approximation used, and α_0 and α_i denote the static polarizabilities in the ground and ith states, respectively. The London approximation would be valid for the excited states if the excitation energy is sufficiently smaller than the ionization potential. For solvatochromic shifts, Bakhshiev proposed an equation that considers the change of dispersive interaction in the ground and excited states in terms of static polarizabilities.[40] In comparison with eq 42, Bakhshiev's equation lacks the second term that is proportional to the square of the transition moment. This term results from the effect of de-excitations on the dispersive interaction in the excited state, and the term is necessary to apply the London approximation to excited states. Equation 42 is similar to the equation obtained by Basu in ref 4.

When the transition moment μ_{0i} is small, such as in the Q-band states, the shift can be explained by the difference in the static polarizabilities. Equation 42 and the calculated static polarizabilities in Table 5 cause the decrease in the Q-band splitting in solution. However, the dispersive interaction is too small to explain the observed large shifts in dipolar and quadrupolar solvents. As shown by the FBP$-(CH_2Cl_2)_2$ model calculations, specific solute−solvent interaction is important for Q-bands. Such interaction could be partly described by the PCM by means of the polarization of the solvent reaction field. For B-band states that have high intensities, the second term on the right-hand side of eq 42 provides the dominant contribution to the solvatochromic shifts.

4.6. QM/MM Model. Previous QM/MM calculations of zinc porphyrin in water reported very small solvatochromic shifts for the $\pi-\pi^*$ excitations.[12,13] In this work, we calculated the explicit solvation model for 22 water molecules with a local minimum conformation obtained using the wB97XD/6-31G** method. The excitation energies were calculated using the TD CAM-B3LYP/D95(d) and LANL2DZ pseudopotential basis sets.[41] The results are shown in Table 6. A remarkable solvent effect was found using our explicit solvation model. The solvatochromic shift for nonpolar solutes cannot be properly described by a conventional QM/MM model, in which the polarization of the MM part induced by electronic transition in the QM is not considered. In contrast, the PCM takes this type of polarization into account. The QM/MM may work for cases where the ground and excited states have significantly different charge distributions, such as in CT excitations. Indeed, the QM/MM model works well for N-band states that are $n-\pi^*$ excitations and have a CT character.[12,13] We also examined a minimal QM model, in which the two nearest water molecules are considered, and the results are shown in Table 6. The distance between the zinc and the water oxygen in this model was 2.326 Å. The calculated solvent shifts by this two water model correspond to 50−65% of the shifts obtained by the model with 22 water molecules.

Table 6. Excitation energies (EE) and solvatochromic shifts (in eV) for zinc porphyrin in water for TD CAM-B3LYP calculations

	in vacuum	shift in water		
state	EE	+ $(H_2O)_{22}$[a]	+ $(H_2O)_2$[a]	QM/MM[b]
$1E_u$	2.351	−0.108	−0.071	+0.01
$1E_u$	2.351	−0.089	−0.053	+0.01
$2E_u$	3.660	−0.213	−0.116	−0.01
$2E_u$	3.660	−0.200	−0.104	0.00

[a]This work, TD CAM-B3LYP/[D95(d), LANL2DZ] calculation with including QM water molecules. [b]Ref 12.

The importance of the polarization of the MM force field was reported by Aidas et al. for $\pi-\pi^*$ excitation of acrolein in water.[42] Their study showed a strong dependence of the $\pi-\pi^*$ excitation on the nonelectrostatic intermolecular interactions. Their result is consistent with our findings and supports the importance of dispersive interactions, even for polar molecules in polar solution. When we consider the polarization of the MM parts, both the LR and SS schemes are available to determine the polarization for the QM excited states. The QM/polarizable MM schemes for electronic excitations will result in a formula similar to those for the PCM of the SS and LR schemes.

5. CONCLUDING REMARKS

In this study, we investigated the origin and mechanism of the solvatochromic shifts of free-base porphine in its $\pi-\pi^*$ excitations as an example of solvatochromic shifts of nonpolar conjugated molecules. We used the SS and LR PCM schemes and explicit solvation models. These models include different types of solute−solvent interactions.

The SS PCM calculations include the difference of electrostatic interaction between the ground and excited states. Such interaction caused hypsochromic shifts for the Q- and B-band states. The LR PCM calculations include an interaction between the solvent and the transition moment, which can be considered as part of the dispersive interaction. The LR PCM calculation reproduced the bathochromic shifts of the B-band states, as did the explicit solvation model. A decomposition analysis showed that this type of transition moment−solvent interaction can be considered using independent particle approximations, such as the CIS approximation. Equation 29,

which is based on the Casimir−Polder formula, would be an appropriate starting point for studying the effect of dispersive interaction on solvatochromic shifts.

The experimental trends in the solvatochromic shifts of FBP can be explained as follows.

1. The observed bathochromic shift of the B-band in solution was attributed to the interaction of transition dipoles with the solvent reaction field. This effect also originated in the dispersive interaction. However, the LR PCM scheme can incorporate this term.

2. The dispersive interaction caused by the polarizability difference between the ground and excited states was an origin of the observed decrease in the Q-band splitting in nonpolar solvents. Many-body theories such as the SAC-CI are necessary to consider this effect.

3. The observed refractive index-dependence of the solvent shifts in *n*-hexane can be explained by the dispersive interactions, which relate to the optical dielectric constants of continuum solvents. The LR PCM can describe this trend well.

4. The remarkable decrease in the Q-band splitting in dipolar and quadrupolar solvents could not be explained by the dispersive interactions alone. As shown by the FBP−$(CH_2Cl_2)_2$ model calculations, specific solute−solvent interactions would be important for the Q-bands, although the dipolar and quadrupolar effects can be partly described by the PCM. Anisotropic interactions would be more important than the geometry relaxation for the decrease in the Q-band splitting in solution. The importance of the electronic structure for the Q-band splitting of free-base phthalocyanines has been reported.[35]

Our computations were performed with only very limited molecular configurations, and molecular vibrations and other thermal effects should be considered for a more precise discussion of the spectroscopic data. The basis functions used may be insufficient for an accurate description of weak intermolecular interactions and induced dipole interactions. However, the essential origins of the solvatochromic shifts can be discussed using our computational results.

The PCM, particularly the LR scheme, and the QM/MM approach are now widely used for studying solvent effects on optical properties. However, this study has shown that the available conventional solvent models seem to be complementary to each other. An essentially important interaction, with a character that depends on the system studied, may be missed if only a single model is used. The SS PCM approach may be better for polar solute molecules, but it is not adequate for nonpolar molecules, such as FBP. The QM/MM approach may work well for systems with specific interactions, such as hydrogen bonds, but it must be applied carefully to the $\pi-\pi^*$ excitations, because it cannot describe nonelectrostatic interactions.

■ ASSOCIATED CONTENT

Supporting Information

The dependence of the solvatochromic shifts on the thresholds of perturbation selection for the PCM SAC-CI calculations, the effect of geometry relaxation, supplemental data for Tables 2 and 3, and the Cartesian coordinates of the model systems. This information is available free of charge via the Internet at http://pubs.acs.org/.

■ AUTHOR INFORMATION

Corresponding Author

*E-mail: fukuda@ims.ac.jp.

Notes

The authors declare no competing financial interest.

■ ACKNOWLEDGMENTS

This work was supported by a Grant-in-Aid for Scientific Research from the Japan Society for the Promotion of Science (JSPS) and the Ministry of Education, Culture, Sports, Science, and Technology (MEXT), Japan; the Strategic Programs for Innovative Research (SPIRE); and the Computational Materials Science Initiative (CMSI). The computations were partly performed in the Research Center for Computational Science, Okazaki, Japan.

■ REFERENCES

(1) Ooshika, Y. *J. Phys. Soc. Jpn.* **1954**, *9*, 594−602.
(2) Longuet-Higgins, H. C; Pople, J. A. *J. Chem. Phys.* **1957**, *27*, 192−194.
(3) McRae, E. G. *J. Phys. Chem.* **1957**, *61*, 562−572.
(4) Basu, S. *Adv. Quantum Chem.* **1964**, *1*, 145−169.
(5) Liptay, W. *Z. Naturforsch.* **1965**, *20a*, 1441−1471.
(6) Bayliss, N. S. *J. Chem. Phys.* **1950**, *18*, 292−296.
(7) Renger, T.; Grundkötter, B.; Madjet, M. El-A; Müh, F. *Proc. Natl. Acad. Sci. U. S. A.* **2008**, *105*, 13235−13240.
(8) Edwards, L.; Dolphin, D. H.; Gouterman, M.; Adler, A. D. *J. Mol. Spectrosc.* **1971**, *38*, 16−32.
(9) Renge, I. *J. Phys. Chem.* **1993**, *97*, 6582−6589.
(10) Renge, I. *Chem. Phys. Lett.* **1991**, *185*, 231−236.
(11) Improta, R.; Ferrante, C.; Bozio, R.; Barone, V. *Phys. Chem. Chem. Phys.* **2009**, *11*, 4664−4673.
(12) Govind, N.; Valiev, M.; Jensen, L.; Kowalski, K. *J. Phys. Chem. A* **2009**, *113*, 6041−6043.
(13) Fan, P.-D.; Valiev, M.; Kowalski, K. *Chem. Phys. Lett.* **2008**, *458*, 205−209.
(14) Cammi, R.; Corni, S.; Mennucci, B.; Tomasi, J. *J. Chem. Phys.* **2005**, *122*, 104513.
(15) Corni, S.; Cammi, R.; Mennucci, B.; Tomasi, J. *J. Chem. Phys.* **2005**, *123*, 134512.
(16) Suramitr, S.; Phalinyot, S.; Wolschann, P.; Fukuda, R.; Ehara, M.; Hannongbua, S. *J. Phys. Chem. A* **2012**, *116*, 924−937.
(17) Cammi, R.; Fukuda, R.; Ehara, M.; Nakatsuji, H. *J. Chem. Phys.* **2010**, *133*, 024104.
(18) Fukuda, R.; Ehara, M.; Nakatsuji, H.; Cammi, R. *J. Chem. Phys.* **2011**, *134*, 104109.
(19) Casimir, H. B. G.; Polder, D. *Phys. Rev.* **1948**, *73*, 360−372.
(20) Frisch, M. J.; Trucks, G. W.; Schlegel, H. B.; Scuseria, G. E.; Robb, M. A.; Cheeseman, J. R.; Scalmani, G.; Barone, V.; Mennucci, B.; Petersson, G. A.; Nakatsuji, H.; Caricato, M.; Li, X.; Hratchian, H. P.; Izmaylov, A. F.; Bloino, J.; Zheng, G.; Sonnenberg, J. L.; Hada, M.; Ehara, M.; Toyota, K.; Fukuda, R.; Hasegawa, J.; Ishida, M.; Nakajima, T.; Honda, Y.; Kitao, O.; Nakai, H.; Vreven, T.; Montgomery, J. A., Jr.; Peralta, J. E.; Ogliaro, F.; Bearpark, M.; Heyd, J. J.; Brothers, E.; Kudin, K. N.; Staroverov, V. N.; Kobayashi, R.; Normand, J.; Raghavachari, K.; Rendell, A.; Burant, J. C.; Iyengar, S. S.; Tomasi, J.; Cossi, M.; Rega, N.; Millam, J. M.; Klene, M.; Knox, J. E.; Cross, J. B.; Bakken, V.; Adamo, C.; Jaramillo, J.; Gomperts, R.; Stratmann, R. E.; Yazyev, O.; Austin, A. J.; Cammi, R.; Pomelli, C.; Ochterski, J. W.; Martin, R. L.; Morokuma, K.; Zakrzewski, V. G.; Voth, G. A.; Salvador, P.; Dannenberg, J. J.; Dapprich, S.; Daniels, A. D.; Farkas, Ö.; Foresman, J. B.; Ortiz, J. V.; Cioslowski, J.; Fox, D. J. *Gaussian 09*, Revision B.01; Gaussian, Inc.: Wallingford, CT, 2010.
(21) (a) Lee, C.; Yang, W.; Parr, R. G. *Phys. Rev. B* **1988**, *37*, 785−789. (b) Becke, A. D. *J. Chem. Phys.* **1993**, *98*, 5648−5652.
(22) (a) Ditchfield, R.; Hehre, W. J.; Pople, J. A. *J. Chem. Phys.* **1971**, *54*, 724−729. (b) Hehre, W. J.; Ditchfield, R.; Pople, J. A. *J. Chem. Phys.* **1972**, *56*, 2257−2261. (c) Hariharan, P. C.; Pople, J. A. *Theor. Chem. Acta* **1973**, *28*, 213−222. (d) Francl, M. M.; Pietro, W. J.;

Hehre, W. J.; Binkley, J. S.; DeFrees, D. J.; Pople, J. A.; Gordon, M. S. *J. Chem. Phys.* **1982**, *77*, 3654−3666.
(23) Chai, J.-D.; Head-Gordon, M. *Phys. Chem. Chem. Phys.* **2008**, *10*, 6615−6620.
(24) Dunning, T. H., Jr.; Hay, P. J. In *Modern Theoretical Chemistry*; Schaefer, H. F., III, Ed.; Plenum Press: New York, 1977; Vol. *3*, pp 1−28.
(25) (a) Perdew, J. P.; Burke, K.; Ernzerhof, M. *Phys. Rev. Lett.* **1996**, *77*, 3865−3868. (b) Perdew, J. P.; Burke, K.; Ernzerhof, M. *Phys. Rev. Lett.* **1997**, *78*, 1396. (c) Adamo, C.; Barone, V. *J. Chem. Phys.* **1999**, *110*, 6158−6169.
(26) Yanai, T.; Tew, D.; Handy, N. *Chem. Phys. Lett.* **2004**, *393*, 51−57.
(27) Nakatsuji, H.; Hada, M.; Ehara, M.; Toyota, K.; Fukuda, R.; Hasegawa, J.; Ishida, M.; Nakajima, T.; Honda, Y.; Kitao, O.; Nakai, H. SAC-CI GUIDE. http://www.qcri.or.jp/sacci/ (accessed Dec 11, 2012).
(28) Fukuda, R.; Nakatsuji, H. *J. Chem. Phys.* **2008**, *128*, 094105.
(29) (a) Cancès, E.; Mennucci, B.; Tomasi, J. *J. Chem. Phys.* **1997**, *107*, 3032−3041. (b) Mennucci, B.; Cancès, E.; Tomasi, J. *J. Phys. Chem. B* **1997**, *101*, 10506−10517.
(30) Marcus, R. A. *J. Chem. Phys.* **1956**, *24*, 979−989.
(31) Cammi, R.; Tomasi, J. *Int. J. Quantum Chem., Symp.* **1995**, *29*, 465−474.
(32) Cammi, R.; Frediani, L.; Mennucci, B.; Tomasi, J.; Ruud, K.; Mikkelsen, K. V. *J. Chem. Phys.* **2002**, *117*, 13−26.
(33) Improta, R.; Barone, V.; Scalmani, G.; Frisch, M. J. *J. Chem. Phys.* **2006**, *125*, 054103.
(34) Even, U.; Jortner, J. *J. Chem. Phys.* **1982**, *77*, 4391−4399.
(35) Fukuda, R.; Ehara, M.; Nakatsuji, H. *J. Chem. Phys.* **2010**, *133*, 144316.
(36) Even, U.; Jortner, J.; Berkovitch-Yellin, Z. *Can. J. Chem.* **1985**, *63*, 2073−2080.
(37) Onsager, L. *J. Am. Chem. Soc.* **1936**, *58*, 1486−1493.
(38) Renge, I.; Wolleb, H.; Spahni, H.; Wild, U. P. *J. Phys. Chem. A* **1997**, *101*, 6202−6213.
(39) London, F. *Trans. Faraday. Soc.* **1937**, *33*, 8−26.
(40) Bakhshiev, N. G. *Opt. Spectrosc.* **1961**, *10*, 379−384.
(41) Hay, P. J.; Wadt, W. R. *J. Chem. Phys.* **1985**, *82*, 270−283.
(42) Aidas, K.; Møgelhøj, A.; Nilsson, E. J. K.; Johnson, M. S.; Mikkelsen, K. V.; Christiansen, O.; Söderhjelm, P.; Kongsted, J. *J. Chem. Phys.* **2008**, *128*, 194503.